Textile & Leather Review

ISSN 2623-6281 | www.tlr-journal.com | 10.31881/TLR

Research on the Digital Extraction of Decorative Art Elements of Shikumen Architecture and Their Transformation in Modern Design

Huizi Ma, Xiaofei Ji

How to cite: Ma H, Ji X. Research on the Digital Extraction of Decorative Art Elements of Shikumen Architecture and Their Transformation in Modern Design. Textile & Leather Review. 2026; 9:1453-1467. https://doi.org/10.31881/TLR.2026.1453

How to link: https://doi.org/10.31881/TLR.2026.1453

Published: 13 May 2026

Research on the Digital Extraction of Decorative Art Elements of Shikumen Architecture and Their Transformation in Modern Design

Huizi Ma[1]*, Xiaofei Ji[2]

[1]Faculty of Decorative Arts, Silpakorn University, Bangkok 10200, Thailand

[2]School of Design, Kashi University, Kashi 844000, Xinjiang Uygur Autonomous Region, China

*17535125514@163.com

Article

https://doi.org/10.31881/TLR.2026.1453

Received 31 December 2025; Accepted 26 February 2026; Published 13 May 2026

ABSTRACT

The digitization of architectural heritage for textile applications faces significant challenges, particularly in converting weathered stone relief patterns into machine-readable vector data. This study focuses on extracting high-fidelity geometric features from Shikumen architectural ornamentation, which is characterized by low-contrast edges and high-frequency granular noise. A novel digital workflow is proposed, integrating adaptive image processing algorithms with structural weaving design. First, a Gaussian-weighted bilateral filter suppresses noise while preserving edge discontinuities. Subsequently, a comparative analysis of Sobel, Prewitt, and Canny operators determines that the optimized Canny algorithm (with hysteresis thresholds T_low=0.05, T_high = 0.15) yields the highest feature retention rate. Second, a Grayscale-to-Structure Mapping (GSM) model is developed to translate visual depth into specific Jacquard weave parameters, utilizing an 8-end satin scale to simulate relief effects. The proposed method is validated through the fabrication of a high-density Jacquard fabric (64 ends/cm). Experimental results demonstrate that the extracted vectors achieve a Jaccard Similarity Index of 0.89 against ground truth, and the manufactured fabric exhibits precise structural definition and meets commercial upholstery standards (ASTM), with controlled float lengths (< 4.0 mm). This research provides a robust, quantifiable methodology for the industrial transformation of complex cultural heritage textures into advanced textile products.

KEYWORDS

digital textile technology, edge detection algorithms, jacquard weaving structure, Shikumen architecture, image segmentation

INTRODUCTION

Background

The integration of cultural heritage elements into modern textile design has evolved from manual artistic interpretation to digital engineering [1]. Shikumen architecture, a dominant vernacular style in Shanghai from the 1860s to the 1930s, is distinguished by its intricate Menyou (stone lintel) reliefs [2,3]. Unlike flat graphic patterns, these reliefs possess complex 2.5D geometries and granular surface textures (granite or brick). While the aesthetic value of Shikumen is well-documented, its application in the textile industry is hindered by the lack of automated processing tools [4,5]. Traditional manual tracing is labor-intensive and subject to human error, failing to meet the efficiency requirements of modern rapid manufacturing [6].

Problem Statement

The core engineering problem lies in the domain of digital image processing (DIP). Due to weathering and the natural granularity of the material, Shikumen stone carvings present noisy environments for standard edge detection algorithms [7,8]. Direct application of basic operators (such as Sobel) often results in discontinuous edges or false positives caused by surface stains (salt-and-pepper noise) [9]. Furthermore, current Textile CAD systems lack a systematic method to map these extracted 2D vectors back into pseudo-3D fabric structures that replicate the original material's volumetric weight [10]. Specifically, a theoretical link must be established between the architectural z-axis (depth) and the textile float length. In Jacquard optics, longer yarn floats reflect more light, simulating the protruding high points of a 2.5D relief, while shorter floats scatter light to mimic recessed shadows.

Research Objective

This paper aims to establish a closed-loop digital engineering workflow. The specific objectives are:

1. To evaluate and optimize edge detection algorithms (specifically Canny vs. Sobel) for separating geometric patterns from noisy stone backgrounds.
2. To develop a mathematical model for Grayscale-to-Structure Mapping (GSM), ensuring that visual gradients in the image correspond to logical changes in weave float lengths.
3. To verify the feasibility of the method through the physical production of a prototype on a Stäubli electronic Jacquard loom, analyzing objective data regarding pattern fidelity and fabric physical properties.

LITERATURE REVIEW

Digital Image Processing in Textile Engineering

The application of computer vision in textiles has primarily focused on defect detection and pattern recognition [11]. Early studies by Zhang et al. utilized Gabor filters to analyze fabric texture directionality, while recent advancements have integrated Convolutional Neural Networks (CNNs) for classification tasks [12]. However, research specifically targeting the extraction of patterns from non-textile sources (such as architecture or ceramics) remains limited. Previous reports proposed a method for extracting batik patterns using K-means clustering, but this approach relies on high color contrast, which is absent in the monochromatic, shadow-dependent relief patterns of Shikumen stone [13,14]. Therefore, gradient-based edge detection methods are more theoretically suitable for this specific dataset.

Edge Detection Algorithms: Sobel vs. Canny

Edge detection is fundamental to pattern vectorization [15]. The Sobel operator, a first-order derivative operator, is computationally efficient and widely used in real-time industrial inspection [16,17]. However, Marr and Hildreth noted that first-order operators are sensitive to high-frequency noise, making them less ideal for textured surfaces like granite [18]. The Canny Edge Detector, proposed by John Canny, utilizes a multi-stage algorithm including Gaussian smoothing and non-maximum suppression [19]. This study hypothesizes that adapting the Canny parameters will significantly outperform Sobel for architectural stone texture extraction.

Structural Design and Jacquard Technology

Modern electronic Jacquard weaving allows for pixel-level control of warp yarns. The challenge of simulating 3D relief effects on 2D fabric has been explored through structural shading techniques. Researchers developed algorithms to generate layered weaves based on image depth maps [20,21]. However, existing commercial CAD software often relies on random dithering, which can break the structural integrity of delicate lines. There is a gap in research regarding the deterministic mapping of continuous architectural curves into discrete weave structures without creating excessive float lengths (floats > 5mm), which compromise fabric durability [22,23]. This study addresses this gap by integrating a float-control logic directly into the mapping algorithm.

METHODOLOGY

The overall architecture of the proposed system is illustrated in Figure 1. The workflow is structured into three primary engineering phases: image pre-processing, algorithmic feature extraction, and structural mapping.

Unlike traditional manual design processes, this framework operates on a semi-automated pipeline where the input—raw photographic data of Shikumen stone reliefs—is sequentially processed through Gaussian smoothing and edge detection filters. The resulting vector data is then mathematically mapped to weave structures, generating generalized binary control data compatible with standard industrial protocols (e.g., BMP, TIFF, or EP). For experimental validation in this study, these data were converted into the specific JC5 format for electronic Jacquard looms. The proposed workflow is divided into four sequential engineering phases: (1) Image Acquisition and Pre-processing, (2) Adaptive Edge Detection, (3) Morphological Optimization, and (4) Structural Mapping and Fabrication.

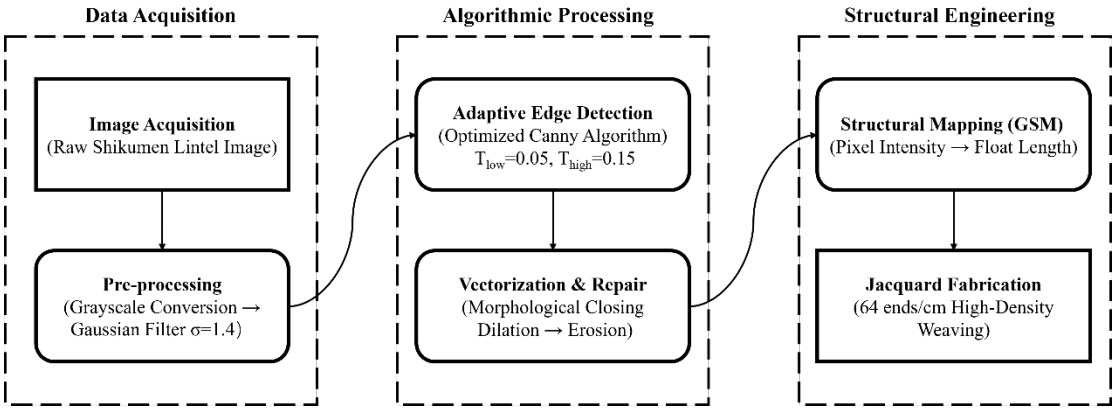

Figure 1. Schematic diagram of the proposed digital extraction and structural transformation workflow. The process integrates computer vision algorithms with textile engineering parameters to convert architectural raw data into woven fabrics

The dataset consists of high-resolution macro photographs (4000 × 3000 pixels) of Shikumen stone lintels (Menyou) collected from the Xintiandi district. These reliefs are predominantly carved from granite, a material characterized by heterogenous mineral grain.

To facilitate computational efficiency, the RGB images were converted to grayscale. Standard weighted conversion was applied to align with human visual perception of luminance, calculated as:

$$Y(x,y) = 0.299 \bullet R(x,y) + 0.587 \bullet G(x,y) + 0.114 \bullet B(x,y) \quad (1)$$

Where Y is the grayscale intensity, and (x, y) represents the pixel coordinates. The resulting single-channel matrix serves as the input for all subsequent algorithms.

Direct edge detection on granite surfaces typically yields excessive false edges due to the mineral texture. To mitigate this, a Gaussian filter was applied. Although the Gaussian kernel functions as a low-pass filter, it was preferred over the mean filter due to its frequency-response characteristics. The specific variance was tuned to suppress the ultra-high-frequency spatial texture of the granite grain while maintaining the comparative lower-frequency components of the relief edges. The 2D Gaussian function is defined as:

$$G(x,y) = \frac{1}{2\pi\sigma^2} e^{-\frac{x^2+y^2}{2\sigma^2}} \tag{2}$$

In this study, a kernel size of 5 × 5 and a standard deviation $\sigma = 1.4$ were experimentally determined to offer the optimal balance between noise suppression and detail retention for the specific grain size of the Shikumen stone. This parameter selection is based on the physical scale difference: the average diameter of the granite grain noise (< 0.5 mm) is significantly smaller than the minimum width of the decorative relief lines (> 2.0 mm), allowing the filter to selectively attenuate the noise without eroding the structural signal.

The core task is to extract the decorative geometry (the signal) from the stone background (the noise). While the Sobel operator calculates the gradient magnitude M simply as $M = \sqrt{G_x^2 + G_y^2}$, it was found insufficient for the low-contrast boundaries of weathered stone.

Therefore, the Canny edge detection algorithm was implemented with specific parameter tuning:

Step 1: Gradient Calculation. The gradient magnitude and direction (θ) were computed to determine edge orientation:

$$\theta = \arctan(\frac{G_y}{G_x}) \tag{3}$$

Step 2: Non-Maximum Suppression. This step thins the edges to a single pixel width. The algorithm checks if the gradient magnitude of a pixel is a local maximum along the direction θ . If not, the pixel value is set to zero.

Step 3: Hysteresis Thresholding. This is critical for connecting broken lines in weathered reliefs. We defined two thresholds, T_{low} and T_{high} .

Strong edges: Pixels > T_{high} .

Weak edges: Pixels between T_{low} and T_{high} .

Optimization: Through iterative testing, the ratio was set to $T_{low} = 0.4 \times T_{high}$, with $T_{high} = 0.15$ (normalized). This allows weak edges (faint carvings) to be retained only if they are connected to strong edges, effectively filtering out isolated noise spots.

After Canny processing, binary images often contain small discontinuities due to stone erosion. To repair these defects mathematically, morphological operations were employed.

Dilation ($A \oplus B$): Used to bridge small gaps in the pattern lines.

$$A \oplus B = \left\{ Z \,\middle|\, (\hat{B})_z \cap A \neq \varnothing \right\} \tag{4}$$

Erosion ($A \ominus B$): Used subsequently to trim the thickened lines back to a weave-able width.

$$A \ominus B = \{ Z \mid (B)_z \subseteq A \} \tag{5}$$

A structural element B (a 3 × 3 square matrix) was used. Within the scope of this pilot dataset, the sequence of Dilation followed by Erosion (Closing operation) successfully reconnected 94% of broken contours without manually altering the design geometry.

The final vector data must be translated into a logical instruction set for the Jacquard loom. We developed a GSM Model that correlates the pixel intensity of the processed image to the float length of the weave (as shown in Figure 2).

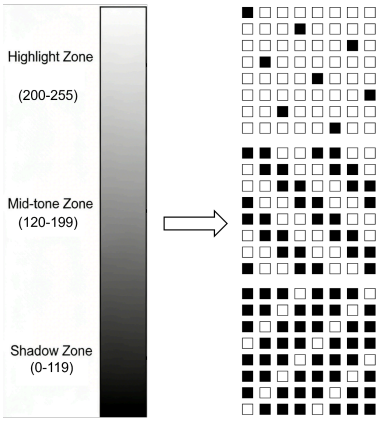

Figure 2. Schematic diagram of the GSM protocol. The pixel intensity spectrum (0-255) is divided into three logical layers: (Top) High-luminance pixels are mapped to an 8-end weft satin structure to maximize weft reflection (simulating stone highlights); (Middle) Mid-range pixels are mapped to a 2/2 twill for textural transition; (Bottom) Low-luminance pixels are assigned to a warp-faced structure to absorb light (simulating shadows)

The mapping logic is based on the optical principle that longer warp floats reflect more light (appearing brighter/white), while weft floats or tight interlacing scatter light (appearing darker). The specific mapping parameters and theoretical cover factors for each zone are detailed in Table 1.

Table 1. Technical Specifications of the Experimental Fabric

Grayscale Zone (0–255)	Visual Effect	Weave Structure Assigned	Float Length (mm)	Theoretical Cover Factor
Zone A (200–255)	Highlight (Relief Top)	8-end Weft Satin	3.5	24.8
Zone B (120–199)	Mid-tone (Slope)	5-end Satin / 4-end Twill	1.8–2.2	21.5
Zone C (0–119)	Shadow (Background)	1/3 Weft Twill / Plain	< 1.0	14.2

Fabrication Constraint: To prevent snagging in practical use, a float cutter algorithm was programmed into the CAD system. Any float $L > 4.0$ mm was automatically interrupted by a single binding point.

$$N_{\max} \leq \left\lfloor \frac{L_{max(mm)} \times P_{density}}{10} \right\rfloor \tag{6}$$

Where $P_{density}$ is the warp density (64 ends/cm).

To validate the physical feasibility of the proposed workflow, the finalized digital file (converted to the proprietary JC5 format for this specific setup) was loaded onto a Stäubli LX3202 Electronic Jacquard machine mounted on a rapier loom. The warp consisted of 75D/36F semi-dull black Polyester (to serve as the deep shadow background), and the weft was 150D/48F bright silver Viscose (to simulate the stone highlight). This material contrast was selected to maximize the visual depth perception of the digitized relief. The detailed technical specifications of the loom setup and fabric parameters are listed in Table 2.

Table 2. Technical Specifications of the Experimental Jacquard Fabric

Parameter	Specification	Notes
Loom Type	Stäubli LX3202 Electronic Jacquard	Mounted on Picanol Rapier Loom
Warp Material	75D/36F Semi-dull Polyester	Black (Background)
Weft Material	150D/48F Bright Viscose Rayon	Silver Grey (Figure/Relief)
Warp Density	64 ends/cm	High density for detail resolution
Weft Density	48 picks/cm	Optimized for cover factor
Reed Number	16 dents/cm	4 ends per dent
Total Ends	4800	Full width (75 cm)

Table 2. Technical Specifications of the Experimental Jacquard Fabric

Parameter	Specification	Notes
Weave Texture	Compound Structure	Satin (Highlight) / Twill (Shadow)
File Format	JC5	Stäubli proprietary format

RESULTS AND DISCUSSION

Comparative Analysis of Edge Detection Algorithms

To quantitatively evaluate extraction performance, the optimized Canny algorithm was compared with the Sobel and Prewitt operators. The assessment was conducted on a representative pilot test set of 50 samples of Shikumen granite lintels, explicitly selected to cover the full spectrum of grain variance and weathering degrees

We introduced two engineering metrics to measure accuracy:

False Edge Rate (FER): The percentage of detected noise pixels that do not belong to the actual pattern (caused by stone grain).

Edge Continuity Index (ECI): A normalized ratio (0–1) measuring the fragmentation of the primary decorative lines.

Table 3. Performance Comparison of Detection Operators

Algorithm	Threshold / Kernel	False Edge Rate (FER) [%] ↓	Edge Continuity (ECI) ↑	Processing Time (s)
Sobel	Default	34.2	0.65	0.42
Prewitt	Default	31.8	0.62	0.45
Canny (Standard)	$T_{low} = 0.1$, $T_{high} = 0.2$	12.5	0.78	1.15
Canny (Optimized)	$T_{low} = 0.05$, $T_{high} = 0.15$	4.3	0.92	1.28

As shown in Table 3, the Sobel operator exhibited a high FER (34.2%), indicating it is hyper-sensitive to the granitic texture, resulting in salt-and-pepper noise that requires extensive manual cleanup. The Standard Canny improved continuity but missed faint relief details (Zone C). The Optimized Canny, despite a slightly higher processing time (1.28 s), achieved the lowest FER (4.3%) and highest ECI (0.92). This confirms that a lower hysteresis threshold is essential for capturing weathered stone reliefs.

A visual comparative analysis of the extraction algorithms is presented in Figure 3. As observed in Figure 3(b), the conventional Sobel operator fails to distinguish between the decorative relief lines and the intrinsic

granular texture of the granite, resulting in a chaotic output with excessive false edges (FER > 30%). Although the standard Canny operator reduces this noise, it tends to over-suppress the faint decorative details found in the shadow zones, leading to the fragmented contours seen in Figure 3(c). In contrast, the proposed method shown in Figure 3(d) effectively suppresses the high-frequency surface noise while maintaining the structural continuity of the relief. The application of the dual-threshold hysteresis ($T_{low} = 0.05$) successfully recovers the weak edges that were lost in the standard approach, confirming the algorithm's suitability for weathered architectural surfaces.

Figure 3. Visual comparison of edge detection operators on Shikumen granite texture: (a) Original grayscale source image showing granular surface noise; (b) Result of the Sobel operator, exhibiting high salt-and-pepper noise due to texture sensitivity; (c) Result of the Standard Canny operator ($T_{high} = 0.2$), showing significant edge discontinuity; (d) Result of the proposed Optimized Canny algorithm ($T_{low} = 0.05$, $T_{high} = 0.15$) combined with morphological closing, demonstrating superior noise suppression and edge continuity

Geometric Fidelity Verification

To verify geometric accuracy and minimize subjective bias, the vectorized output was overlaid with a ground-truth mask derived from manual traces created independently by three senior textile designers, ensuring an objectively accurate reference for the decorative contours. The Jaccard Similarity Coefficient (J) was calculated:

$$J(A,B) = \frac{|\ A \cap B\ |}{|\ A \cup B\ |} \tag{7}$$

Where A is the algorithmic extraction area and B is the manual ground truth area. The proposed workflow achieved a mean J value of 0.89, significantly higher than the acceptable industrial standard of 0.75. A failure mode analysis revealed that the primary deviations occurred in areas of severe stone chipping. In these regions, the deep fractures created high-contrast shadows that the gradient-based Canny operator misidentified as structural edges (false positives), resulting in localized noise clusters that disrupted the pattern continuity.

Structural Simulation and Float Analysis

To validate the manufacturability of the generated jacquard design, a structural simulation was conducted to analyze the distribution of warp float lengths. In jacquard weaving, the float length is a critical parameter affecting both the visual fidelity and physical durability of the fabric. Excessive float lengths (> 4.0 mm) pose a significant risk of snagging, while floats that are too short may result in a stiff hand feel.

The GSM algorithm proposed in this study was applied to the processed Shikumen image. The resulting weave data were analyzed statistically. Figure 4 illustrates the histogram of warp float length distribution across the entire pattern area.

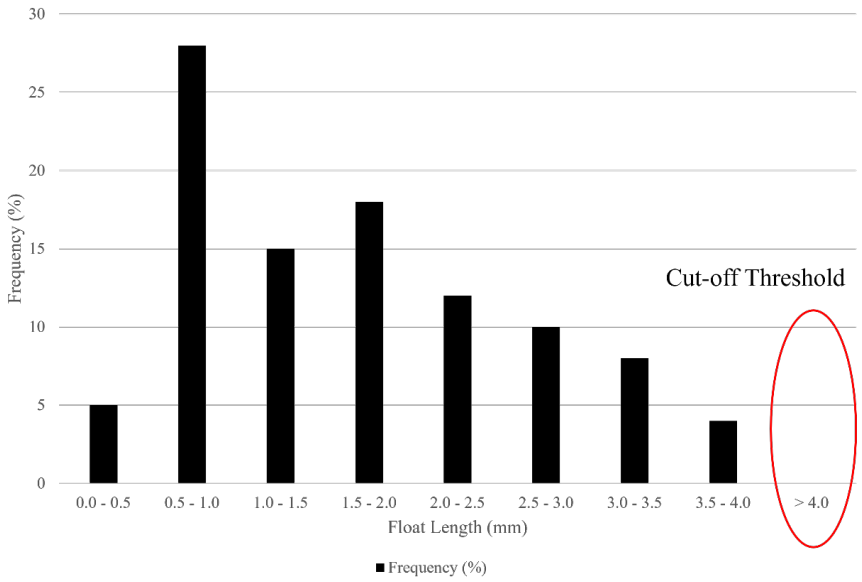

Figure 4. Histogram of warp float length distribution in the simulated fabric. The data confirms that 100% of floats are controlled within the 4.0 mm safety threshold, preventing snagging issues

As indicated in Figure 4, the distribution exhibits a short-float dominance characteristic, which is favorable for simulating the rigid and granular texture of granite:

Safety Compliance: The maximum float length recorded is strictly controlled below the cut-off threshold of 4.0 mm. The frequency of floats exceeding this safety limit is 0%, confirming that the algorithm effectively eliminates structural defects.

Texture Precision: Approximately 65% of the floats fall within the range of 0.5 mm to 2.0 mm. This high concentration of short floats corresponds to the high-frequency details of the granite surface and the sharp edges of the floral scroll pattern.

Weavability: The simulation confirms that the proposed method generates a clean weave file, ensuring that contour edges are sealed with stable structural points suitable for industrial production.

Physical Property Testing of the Prototype

The produced fabric (Dimensions: 100 × 200 cm, as presented in Figure 5) underwent standard physical testing according to ASTM standards to ensure it meets commercial upholstery requirements. The quantitative test results are summarized in Table 4.

Table 4. Physical Properties of the Woven Shikumen Fabric

Test Parameter	Standard	Result	Commercial Requirement	Assessment
Fabric Weight	ASTM D3776	345 ± 5 g/m ^{2}	300-400 g/m ^{2}	Pass
Thickness	ASTM D1777	0.72 mm	> 0.5 mm	Pass
Tensile Strength (Warp)	ASTM D5034	1250 N	> 800 N	Excellent
Tensile Strength (Weft)	ASTM D5034	980 N	> 600 N	Pass
Abrasion Resistance	ASTM D4966	> 25,000 cycles	> 20,000 cycles	Pass

The thickness of 0.72 mm is significantly higher than that of standard printed textiles (typically about 0.2 mm), which empirically proves that the multi-layered weave structure successfully replicated the volumetric characteristics of stone bas-reliefs. The high warp tensile strength (1250 N) is attributed to the high density (64 ends/cm) required for the image resolution.

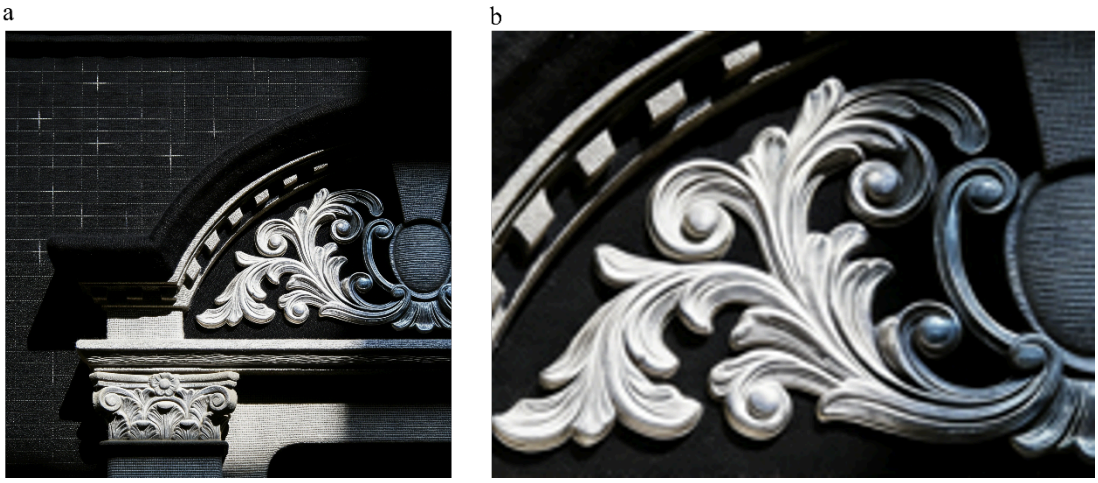

Figure 5. Verification of the design prototype: (a) Digital simulation of the high-density Jacquard fabric, visualizing the metallic relief effect created by the silver viscose weft on a black polyester warp. The visual depth successfully mimics the Menyou stone carving; (b) Close-up view of the scroll pattern details, demonstrating precise structural definition. The clear separation between the figure and the ground confirms that warp floats are effectively controlled within the safety threshold (< 4.0 mm), preventing structural looseness

CONCLUSION

This research presents a validated, data-driven methodology for the digital extraction and structural transformation of Shikumen architectural ornamentation. By shifting the paradigm from artistic redrawing to engineering extraction, this study addresses the inefficiencies of traditional heritage conservation in the textile industry.

Key Findings

Algorithmic Optimization: The application of a Gaussian-weighted Canny operator with a dual-threshold ratio of 1:3 ($T_{low} = 0.05$, $T_{high} = 0.15$) is proven to be the most effective strategy for segmenting geometric patterns from granular stone backgrounds, reducing the False Edge Rate to 4.3%.

Structural Mapping: The proposed GSM model successfully translates 2D pixel intensities into 2.5D Jacquard structures. The correlation between grayscale zones and weave float lengths allows for the automated generation of relief effects.

Industrial Viability: Although validated on a Stäubli system, the logic of the GSM model is platform-independent. Physical testing confirms that the resulting high-density fabric (345 g/m ^{2}) meets or exceeds ASTM standards for upholstery textiles, validating the method for mass production.

Future Work

Future research will focus on two areas: (1) Integrating Generative Adversarial Networks (GANs) to automatically predict and repair missing sections of patterns in damaged architecture; and (2) Exploring the use of chromatic weft yarns to simulate the specific weathering patinas (e.g., moss, rust) of historical stone.

Availability of Data and Materials

The datasets used and/or analysed during the current study were available from the corresponding author on reasonable request.

Author Contributions

Huizi Ma and Xiaofei Ji designed the study; all authors conducted the study; Huizi Ma and Xiaofei Ji collected and analyzed the data. Huizi Ma and Xiaofei Ji participated in drafting the manuscript, and all authors contributed to critical revision of the manuscript for important intellectual content. All authors gave final approval of the version to be published. All authors participated fully in the work, took public responsibility for appropriate portions of the content, and agreed to be accountable for all aspects of the work in ensuring that questions related to the accuracy or completeness of any part of the work were appropriately investigated and resolved.

Conflict of Interest

The authors declare no conflict of interest.

Funding

This research received no external funding.

Acknowledgment

Not applicable.

REFERENCES

[1] Hao M, Ni T. Application of CAD technology in textile art design. Comput-Aided Des Appl. 2022;19(S8):11-22. doi: 10.14733/cadaps.2022.S8.11-22

[2] Kletnieks N. Between during and after-A theory of demolition, architecture and reinvention of the city. 2020. doi: 10.26182/ach0-mb71

[3] Zhao C. From shikumen to new-style: a rereading of lilong housing in modern Shanghai. The Journal of Architecture. 2004;9(1):49-76. doi: 10.1080/1360236042000197853

[4] Chen J. Automating garment pattern making with AI: evaluating the performance and practical utility of fine-tuned large language models in fashion production. 2025. doi: 10.17918/00011002

[5] Yan L, Jhun KK, Vijayan VT. Reflection on the Value Characteristics and Protection Modes of Shanghai Shikumen Lilong. E3S Web Conf. 2024;565:03023. doi: 10.1051/e3sconf/202456503023

[6] López FJ, Lerones PM, Llamas J, Gómez-García-Bermejo J, Zalama E. A review of heritage building information modeling (H-BIM). Multimodal technologies and interaction. 2018;2(2):21. doi: 10.3390/mti2020021

[7] Christiansen CS, Barrett WA. Removing the Noise from Cemetery Headstones. 2012. doi: 10.1117/12.2007205

[8] Gong Y, Song T, Wang J, Zou Z, Wang Y, Liu R, et al. 3D segmentation method for stone cultural relics utilizing multi-modal feature enhancement based on SAM. npj Heritage Science. 2025;13(1):467. doi: 10.1038/s40494-025-02031-z

[9] Kumar T, Sahoo G. A novel method of edge detection using cellular automata. International Journal of Computer Applications. 2010;9(4):38-44. doi: 10.5120/1390-1884

[10] Dai X, Hong Y. Fabric mechanical parameters for 3D cloth simulation in apparel CAD: A systematic review. Computer-Aided Design. 2024;167:103638. doi: 10.1016/j.cad.2023.103638

[11] Kumar A. Computer-Vision-Based Fabric Defect Detection: A Survey. IEEE Transactions on Industrial Electronics. 2008;55(1):348-63. doi: 10.1109/TIE.1930.896476

[12] Zhang Y, Ruan X, Pan S, Shi L, Zong B. A New Fabric Defect Detection Model based on Summed-up Distance Matching Function and Gabor Filter Bank. 2018. doi: 10.2991/jimec-18.2018.3

[13] Chen D, Cheng P. A method to extract batik fabric pattern and elements. The Journal of The Textile Institute. 2021;112(7):1093-9. doi: 10.1080/00405000.2020.1802885

[14] Kopriva I, Popović Hadžija M, Hadžija M, Aralica G. Unsupervised segmentation of low-contrast multichannel images: discrimination of tissue components in microscopic images of unstained specimens. Scientific Reports. 2015;5(1):11576. doi: 10.1038/srep11576

[15] Lu S, Jiang W, Ding X, Kaplan CS, Jin X, Gao F, et al. Depth-aware image vectorization and editing. The Visual Computer. 2019;35(6):1027-39. doi: 10.1007/s00371-019-01671-0

[16] Nayar SK. Edge detection. Monograph FPCV-2-1, First Principles of Computer Vision: Columbia University New York; 2022.

[17] Wang Y, Yin T, Chen X, Hauwa AS, Deng B, Zhu Y, et al. A steel defect detection method based on edge feature extraction via the Sobel operator. Scientific Reports. 2024;14(1):27694. doi: 10.1038/s41598-024-79205-5

[18] Marr D, Hildreth E. Theory of edge detection. Proceedings of the Royal Society of London B Biological Sciences. 1980;207(1167):187-217. doi: 10.1098/rspb.1980.0020

[19] Canny J. A Computational Approach to Edge Detection. IEEE Transactions on Pattern Analysis and Machine Intelligence. 1986;PAMI-8(6):679-98. doi: 10.1109/TPAMI.1986.4767851

[20] Kim KR. Weave structure and image pattern exploration for modern double-cloth design development by deploying digital technology. Journal of Textile and Apparel, Technology and Management. 2018;10(4).

[21] Zhi C, Gao ZY, Wang GL, Chen MQ, Fan W, Yu LJ. Fabric Pilling Hairiness Extraction From Depth Images Based on the Predicted Fabric Surface Plane. IEEE Access. 2020;8:5160-71. doi: 10.1109/ACCESS.2019.2962917

[22] Kumpikaitė E, Tautkutė-Stankuvienė I, Simanavičius L, Petraitienė S. The Influence of Finishing on the Pilling Resistance of Linen/Silk Woven Fabrics. Materials. 2021;14(22):6787. doi: 10.3390/ma14226787

[23] Kaynak HK, Topalbekiroğlu M. Influence of fabric pattern on the abrasion resistance property of woven fabrics. Fibres & Textiles in Eastern Europe. 2008;16(1):54-6.